HHS Public Access

Author manuscript

Adv Redox Res. Author manuscript; available in PMC 2022 December 21.

Published in final edited form as:

Adv Redox Res. 2022 December ; 6: . doi:10.1016/j.arres.2022.100051.

Obese female mice do not exhibit overt hyperuricemia despite hepatic steatosis and impaired glucose tolerance

Sara E. Lewis[d], **Lihua Li**[a], **Marco Fazzari**[a], **Sonia R. Salvatore**[a], **Jiang Li**[b], **Emily A. Hileman**[d], **Brooke A. Maxwell**[d], **Francisco J. Schopfer**[a,c], **Gavin E. Arteel**[b,c], **Nicholas K.H. Khoo**[a,c,1,*], **Eric E. Kelley**[d,1,**]

[a]Department of Pharmacology & Chemical Biology, USA

[b]Division of Gastroenterology, Hepatology and Nutrition, USA

[c]Pittsburgh Liver Research Center, University of Pittsburgh, Pittsburgh, PA 15261, USA

[d]Department of Physiology and Pharmacology, School of Medicine, West Virginia University, 3072B Health Sciences Center, PO Box 9229, Morgantown, WV 26506-9229, USA

Abstract

Recent reports have clearly demonstrated a tight correlation between obesity and elevated circulating uric acid levels (hyperuricemia). However, nearly all preclinical work in this area has been completed with male mice, leaving the field with a considerable gap in knowledge regarding female responses to obesity and hyperuricemia. This deficiency in sex as a biological variable extends beyond unknowns regarding uric acid (UA) to several important comorbidities associated with obesity including nonalcoholic fatty liver disease (NAFLD). To attempt to address this issue, herein we describe both phenotypic and metabolic responses to diet-induced obesity (DIO) in female mice. Six-week-old female C57BL/6J mice were fed a high-fat diet (60% calories derived from fat) for 32 weeks. The DIO female mice had significant weight gain over the course of the study, higher fasting blood glucose, impaired glucose tolerance, and elevated plasma insulin levels compared to age-matched on normal chow. While these classic indices of DIO and NAFLD were observed such as increased circulating levels of ALT and AST, there was no difference in circulating UA levels. Obese female mice also demonstrated increased hepatic triglyceride (TG), cholesterol, and cholesteryl ester. In addition, several markers of hepatic inflammation were significantly increased. Also, alterations in the expression of redox-related enzymes were observed in obese mice compared to lean controls including increases in extracellular superoxide dismutase (Sod3), heme oxygenase (Ho)-1, and xanthine dehydrogenase (Xdh). Interestingly, hepatic UA levels were significantly elevated (~2-fold) in obese mice compared to their lean counterparts.

[*]Corresponding author at: Department of Pharmacology & Chemical Biology, University of Pittsburgh, 200 Lothrop Street, E1340 Thomas E. Starzl Biomedical Science Tower, Pittsburgh, PA 15261, nkhoo@pitt.edu (N.K.H. Khoo). [**]Corresponding author: eric.kelley@hsc.wvu.edu (E.E. Kelley).

[1]These authors contributed equally to this work.

Declaration of Competing Interest

We have no conflict of interest.

Supplementary materials

Supplementary material associated with this article can be found, in the online version, at doi: 10.1016/j.arres.2022.100051.

These data demonstrate female mice assume a similar metabolic profile to that reported in several male models of obesity in the context of alterations in glucose tolerance, hepatic steatosis, and elevated transaminases (ALT and AST) in the absence of hyperuricemia affirming the need for further study.

Keywords

Uric acid; Xanthine oxidoreductase; Female mice; Diet-induced obesity; Hepatic steatosis; Impaired glucose tolerance

Introduction

Obesity is a critical healthcare issue associated with metabolic syndrome and several comorbidities including, but not limited to, diabetes, vascular dysfunction, and fatty liver disease. As such, there has been considerable effort extended to identify primary mechanisms and targetable pathways for intervention and treatment. One such pathway is uric acid (UA) metabolism, as numerous studies have shown that hyperuricemia (high UA levels) is a strong independent predictor of obesity [1–6]. However, these studies fall short of determining causation versus correlation and do not address whether there is a sex difference in circulating UA.

While a small number of reports addressing diet-induced obesity (DIO) clearly indicate disparity between male and female mice in terms of weight gain and impaired glucose tolerance, many reports do not investigate physiologic differences in females that potentially impact the metabolic consequences of obesity that have been extensively defined in males. The role of hyperuricemia in DIO is one area which has not been examined in females. In male rodents, elevated UA levels have been tightly associated with obesity and proposed to propagate metabolic syndrome [7–14]. This potential relationship is evidenced by several reports in various male models of murine obesity and type II diabetes (T2D) indicating a causal role for UA in insulin resistance and hepatic steatosis. Moreover, pharmacologic inhibition of UA synthesis or clearance produces beneficial metabolic outcomes [7–14]. While these studies do employ various models of obesity or metabolic syndrome including genetic alterations in leptin signaling, high-fat and/or high fructose diets, they do not meet with universal agreement. For example, we have previously shown that C57BL/6J male mice fed the 60% HFD had overt hyperuricemia (> 6 mg/dL); and ablation of hyperuricemia failed to improve insulin resistance and/or impaired glucose tolerance in these obese male mice [15]. Therefore, regardless of the current debate (causation versus correlation), the consistent observation is that male mice demonstrate hyperuricemia concomitant with obesity and metabolic syndrome. While some clinical data suggest hyperuricemia is also associated with adolescent and adult obesity in females [16], little, if any, data exists describing UA levels in obese female mice.

Consistent with the absence of data regarding UA levels in female murine obesity, studies regarding nonalcoholic fatty liver disease (NAFLD) or nonalcoholic hepatic steatosis (NASH) are also generally limited to male mice. In fact, a recent review was honest in

pointing out that the sex differences in NAFLD are lagging behind other areas of research in terms of the number of publications including adiposity, metabolic syndrome, and T2D [17].

Herein we address a critical need in the field by assessing the impact of DIO on phenotypic and metabolic outcomes in female mice with a focus on NAFLD/NASH. Numerous studies [7–14], including our own [15], clearly demonstrate obese male mice derived from both diet-induced and genetic strategies are hyperuricemic. To conform with the reduction in numbers ascribed by federal guidelines regarding the use of animals in research, herein we specifically focus on female mice. We report normal UA levels in obese C57BL/6J female mice: an observation critical to advancing our understanding of key biomarkers and potential pharmacologic targets for addressing obesity and its allied comorbidities.

Materials and methods

Mouse model

All animal studies were conducted under the approval of the West Virginia University and University of Pittsburgh Institutional Animal Care and Use Committee (protocol# 1707008288 and 20016708, respectively). Female C57BL/6J mice were purchased from Jackson Laboratory (Bar Harbor, ME). Mice were housed on a 12 h light/dark cycle. Obesity was induced by the HFD (D12492, with 60% of the adjusted calories derived from fat, 20% protein, and 20% carbohydrate) for 32 wk beginning at age 5, 6 wk. Age-matched controls (n = 10) were fed a grain-based diet consisting of adjusted calories derived from 18% fat, 24% protein, and 58% carbohydrate obtained from Envigo Diets (2018 Teklad Global 18% Protein Rodent Diet; Madison, WI). Diet and water were supplied *ad libitum* for the entire study. Mouse weight was recorded weekly.

Blood and tissue collection

At week 23 on the diets, blood was collected from all mice for plasma XO and UA activity. Briefly, local anesthetic was applied to the tail and a small nick was made to collect blood. Blood was immediately spun at 8600 × g for 10 min at 4 °C and plasma was placed in a separate tube and snap frozen. At week 32, mice were weighed, euthanized, and tissues and blood were collected. Tissues were immediately snap frozen in liquid nitrogen and blood was collected by cardiac puncture as previously described [18].

Uric acid detection

Tissues were homogenized in RIPA buffer with protease inhibitor cocktail and briefly spun down. Both tissue and plasma samples were processed as described below with sample volumes as follows: 10 μl for tissue and 5 μl for plasma. Potential urate oxidase (uricase) activity was inhibited by the addition of oxonic acid (100 μM) to ensure UA levels were not altered and thus enzyme activity was not underestimated. Total UA production in 60 min at 37 °C in the presence of xanthine (75 μM) served as the basis for the quantification of total xanthine oxidoreductase (XOR) activity. To ensure XO dependence on urate formation as well as establish base-line UA levels, allopurinol (100 μM) was used in parallel samples to inhibit XOR. Following incubation for 60 min at 37 °C, protein was precipitated with ice cold acetonitrile. The samples were then centrifuged for 12 min at 13,200 × g, at 4 °C.

Following centrifugation, the supernatant was removed, placed in borosilicate glass tubes, dried (60 min), and resuspended in isocratic mobile phase (300 μL) and filtered through a 0.20 μm nylon membrane filter unit into 11 mm plastic snap top auto-sampler vials. The UA content was measured by electrochemical detection (Vanquish UltiMate 3000 ECD-3000RS) coupled to reverse-phase HPLC using a C18 column (150 × 4.6 mm, 3 μm particle size, Luna Phenomenex) and isocratic mobile phase (50 mM sodium dihydrogen phosphate, 4 mM dodecyltrimethylammonium chloride, 2.5% methanol, pH 7.0). Plasma UA activity was denoted as mg/dL and tissue UA activity was denoted as nmol/mg protein.

Glucose tolerance tests

Mice were fasted for 5 h and a glucose tolerance test (GTT) was performed as previously described [19]. Body weight was measured using a precision scale.

Blood chemistry assays

Blood was collected by cardiac puncture during sacrifice under isoflurane anesthesia using heparinized syringes and was kept on ice until centrifugation at 8600 × g for 10 min at 4 °C for plasma isolation. Transaminases (aspartate, AST and alanine, ALT) were determined spectrophotometrically using standard kits (ThermoFisher Scientific; Waltham, MA), as described previously [20]. Insulin levels were determined using an insulin rodent chemiluminescence enzyme-linked immunosorbent assay according to the manufacturer's specifications.

Hepatic triglyceride measurements

Triglycerides (TG) were extracted from ~15 mg liver powder with 200 μl ethyl acetate spiked with 21.2 pmol triheptadecanoin (Nu-Chek Prep., Inc.) as internal standard. Samples were vortexed and centrifuged for 5 min at 15,000 g at 4 °C. Supernatant was diluted in acetonitrile/ethylacetate (50/50, v/v) and TG were analyzed by HPLC-High Resolution (HR)-MS/MS as previously described [18]. Briefly, HPLC-HR-MS/MS analysis of TG was performed using a C8 Luna column (2 × 150 mm, 5 μm, Phenomenex) with a flow rate of 0.4 ml/min and mobile phases of acetonitrile/water (9:1, v/v) 0.1% ammonium acetate (solvent A) and isopropanol/ acetonitrile 0.1% ammonium acetate (7:3, v/v) (solvent B). The gradient program was the following: 35–100% solvent B (0.1–10 min), 100% solvent B (10–13 min), followed by 4 min of re-equilibration to initial conditions. A Q-Exactive hybrid quadrupoleorbitrap mass spectrometer (ThermoFisher) was used in positive mode with the following parameters: auxiliary gas heater temperature 250 °C, capillary temperature 300 °C, sheath gas flow rate 20, auxiliary gas flow rate 20, sweep gas flow rate 0, spray voltage 4 kV, S-lens RF level 60 (%). Full mass scan analysis ranged from 700 to 1500 m/z at 17,500 resolution.

Lipid extraction for cholesterol analysis

Liver tissue homogenates were spiked with d_7-Cholesterol and 16:0-d_7-cholesteryl ester (Avanti Polar Lipids, Al) as internal standards. Lipids were extracted by adding 1 mL of diethyl ether and vortexed. The organic phase was transferred to a clean vial, dried under nitrogen, and reconstituted in 100 μl of chloroform/methanol (20/80 v/v) for mass

spectrometry analysis. *HPLC-MS.* Cholesterol and cholesteryl esters were resolved using a C18 column (100 × 2 mm, 5 μm particle size; Luna Phenomenex) at a 700 μl/min flow rate with a gradient solvent system consisting of solvent A: water/ acetonitrile/ formic acid (50/50/0.1 v/v/v) and solvent B: isopropanol/ acetonitrile/ formic acid (90/10/0.1 v/v/v). Samples were applied to the column at 50% B and eluted with a linear increase in solvent B over 8 min (50–100% B). The gradient was held at 100% B for 2 min and then returned to equilibration conditions for 3 min. The cholesterol and total cholesteryl esters were determined from analyte/internal standard area ratios using an AB5000 or Qtrap 6500 plus triple quad mass spectrometer (Absciex, MA) in positive ion mode with the following setting: collision gas set at 5 units, curtain gas at 40 units, ion source gas number 1 at 60 units and number 2 at 45 units, ion spray voltage at 5500 V, and temperature at 650 °C. The declustering potential was 80 eV, entrance potential 5 eV, collision energy 30 eV, and the collision exit potential 10 eV. Under these conditions, cholesterol esters fragment in the source during ionization, leading to the detection of positively charged cholesterol for all peaks. Signals corresponding to cholesterol and cholesterol esters (detected as cholesterol showing delayed retention times were integrated to obtain the corresponding area under the curve). The following MRM transitions were monitored: 369/161 for cholesterol and cholesteryl ester and MRM: 376/161 for d_7-cholesterol and 16:0-d_7-cholesteryl ester.

Western blotting

Liver samples were pulverized to a fine powder under dry ice conditions using the Cellcrusher (Cell Crusher, Schull, Ireland). The liver powder was homogenized in RIPA buffer. The protein concentration was determined by the BCA protein assay kit (Pierce, Rockford, IL). Protein was denatured by boiling, resolved by SDS-PAGE, and transferred to nitrocellulose (BioRad, Hercules, CA). All membranes were probed with primary antibody (1:1000 dilution) overnight at 4 °C. The following primary antibodies were purchased from Cell Signaling Technology (Danvers, MA) unless otherwise noted: p-Acetyl-CoA Carboxylase (p-ACC @Ser79; D7D11, Rabbit mAb #11818), ACC (C83B10; Rabbit mAb #3676), p-ATP-Citrate Lyase (p-Acl @Ser455; Rabbit Ab #4331), Acl (Rabbit Ab #4332), Fatty Acid Synthase (Fasn; C20G5, Rabbit mAb #3180), Mn-SOD (Sod2; D3 × 8F, Rabbit mAb #13141), IL-1 beta (Il-1 β; P420B, Rabbit Ab; ThermoFisher), and Xanthine Dehydrogenase/Xanthine Oxidase (Xdh/Xo; A-3, mouse mAb sc-398548; Santa Cruz Biotechnology, Dallas, TX). Following the overnight incubation with primary antibody, the membranes were washed several times with TTBS, and then incubated with horseradish peroxidase-conjugated antibodies at 1:10,000 dilution. Immunoreactive bands were detected using chemiluminescence (Bio-Rad). To verify protein loading, membranes were subsequently stripped and re-probed with glyceraldehyde 3-phosphate dehydrogenase (Gapdh; 14C10, Rabbit mAb #2118) purchased from Cell Signaling Technology.

Quantitative real-time PCR

Total RNA was extracted using TRIzol reagent (Invitrogen, Carlsbad, CA, USA). RNA was reverse-transcribed using the iScript cDNA synthesis kit (BioRad, Hercules, CA, USA) as previously described [18]. Gene expression was determined by quantitative real-time (RT)-PCR (qPCR) using TaqMan gene expression assays-on-demand (Applied Biosystems, Foster City, CA, USA) and normalized to *Actin* using the comparative Ct method. Gene

expression stability analyses using four normalization algorithms (Delta CT, BestKeeper, Normfinder, and Genorm) deemed *Actin* as the most suitable housekeeping gene to use for all HFD and NC liver samples.

Statistical analysis

All statistical analyses were performed using Prism 9.1.2 (GraphPad, San Diego, CA). Data were expressed as mean ± SEM and all distributions were tested for normality and homoscedasticity. Data were analyzed by one-way analysis of variance (ANOVA) with Tukey's multiple comparison or Student's t-test post hoc comparisons unless otherwise specified. Differences between groups with $p < 0.05$ were deemed significant. Data outliers were identified using the ROUT method with a maximum false discovery rate (Q value) of 2%. No exclusion criteria were pre-established.

Results

HFD-fed female mice gained weight and had impaired glucose tolerance

Female mice fed a HFD gained weight compared with age-matched mice on normal chow (NC). By week 9, there was a significant increase in weight gain in the HFD-fed group compared to age-matched on NC (Fig. 1A, 2-way ANOVA using Šídák's multiple comparisons test). Overall, the total body weight gain for the female mice on the HFD after 32 weeks of feeding was 33.5 g compared to 11.6 g on the NC (Fig. 1B). At week 30, an intraperitoneal glucose tolerance test (GTT) was performed. Female mice fed a HFD had impaired glucose tolerance compared to the age-matched NC controls (Fig. 2A). There was a significant increase in fasting blood glucose (FBG) levels, at $t = 0$ of the GTT, in the HFD mice (shaded) compared to NC (open) (Fig. 2B, 180.4 ± 4.9 vs 150.5 ± 6.3, $p = 0.0009$). Additionally, the weights of the mice were recorded the day of the GTT as indicated in Fig. 2C.

Transaminases, insulin, and UA profile at week 32

Plasma ALT and AST levels were significantly higher in the HFD-fed group compared to the NC controls at the terminal blood draw (Fig. 3A). Plasma insulin levels were 9.6-fold higher in the HFD-fed female mice (5.2 ± 0.84 ng/mL) versus the NC group (0.54 ± 0.17 ng/mL, Fig. 3B). However, plasma UA levels were slightly increased in the HFD-fed female mice, but did not reach statistical significance (Fig. 3C, $p = 0.0667$; unpaired two-tailed Student's t-test), compared to the age-matched NC-controls. Interestingly, there is a significant correlation between plasma UA levels and weight (Fig. 3D, $p = 0.0236$; $R^2 = 0.1546$) as well as plasma UA and delta weight (Fig. 3E, $p = 0.02$; $R^2 = 0.1675$).

HFD increased hepatic UA, triglyceride, cholesterol, and cholesteryl esters

While the plasma UA levels did not reach significance between the two groups, the female mice fed a HFD for 32 weeks resulted in a significant increase in hepatic UA levels (0.74 ± 0.07 nmol/mg protein) compared to NC controls (0.35 ± 0.08 nmol/mg protein, Fig. 4A). Hepatic triglyceride (TG) levels were markedly increased in the HFD group (Fig. 4B). Additionally, total hepatic cholesterol (Fig. 4C) and cholesteryl esters (Fig. 4D) were significantly higher in the female mice fed the HFD for 32 weeks compared to age-matched

on NC. Again, there is a significant correlation between hepatic UA levels vs body weight (Fig. 4E, $p = 0.043$; $R^2 = 0.134$) and delta body weight (Fig. 4F, $p = 0.042$; $R^2 = 0.135$). However, there is no correlation with hepatic UA levels and liver weight (Fig. 4G, $p = 0.157$; $R^2 = 0.068$).

Hepatic mRNA profile of HFD-fed female mice

The steady-state mRNA expression levels of hepatic proinflammatory genes interleukin-1 β (*Il1b*), monocyte chemoattractant protein-1 (*Ccl2*), and tumor necrosis factor-alpha (*Tnfa*) were increased in the female mice fed the HFD compared to NC. Additionally, macrophage markers *Cd68* and *F4/80* mRNA levels were increased in the HFD group. Significant increases in the mRNA expression of genes involved in reactive oxygen and nitrogen species generation/redox signaling responses including heme oxygenase-1 (*Ho1*), endothelial nitric oxide synthase (*Nos3*), superoxide dismutase-3 (*Sod3*), and xanthine dehydrogenase (*Xdh*) were observed in the female HFD group compared to the NC controls. Despite increased hepatic TG, cholesterol, and cholesteryl esters observed in the HFD group along with an increase in hepatic adipose fatty acidbinding protein (*aP2*) mRNA expression, genes responsible for lipogenesis (*Acaca*, *Acyl*, *Fasn*, *Scd1*, *Scd2*) were not changed. Intriguingly, genes responsible for the mobilization of fatty acids (FA), fatty transporter *Cd36* and lipoprotein lipase (*Lpl*), were increased in the HFD group. This potential increase in hepatic FA mobilization was met with greater expression of acyl-coenzyme A oxidase (*Acox*), which is responsible for FA oxidation of very long-chain fatty acids in the peroxisome, in the HFD-fed female mice. Additionally, genes involved in hepatic gluconeogenesis (indicated by the abbreviation **G**) were increased in the HFD- compared to NC-fed female mice, with *G6pc* reaching significance. Interestingly, fibrotic markers collagen type I alpha-1 (*Col1a1*) and -2 (*Col1a2*), platelet-derived growth factor subunit B (*PdgfB*), transforming growth factor-beta (*Tgfb*), and to a lesser extent smooth muscle actin (*Acta*) were expressed higher in the livers from the HFD group compared to the female mice fed NC. Lastly, the transcription factors fibroblast growth factor 21 (*Fgf21*), peroxisome proliferator-activated receptor gamma coactivator 1-alpha (*Pgc1a*), and sterol regulatory element-binding protein 1 (*Srebp1*) had higher mRNA expression levels in the HFD group. These three genes have key roles in the transcriptional regulation of liver metabolism and homeostasis under physiological conditions. However, these transcription factors also have been implicated in the initiation and progression of NAFLD and NASH [21–23]. In general, this hepatic mRNA profile indicates that DIO-female mice have increased expression of genes associated with inflammation, FA metabolism, fibrosis, gluconeogenesis, and redox/antioxidants while there is no significant change or a decrease in genes associated with the de novo lipogenesis pathway (Fig. 5).

Hepatic protein profile of HFD-fed female mice

With the increase in hepatic TG, cholesterol, and cholesteryl esters in the HFD group, it was surprising to observe a significant decrease in proteins that regulate lipogenesis. After normalization to GAPDH, the HFD group had significantly lower protein expression of ACL ($p = 0.023$), p-ACC ($p < 0.0001$), ACC ($p < 0.0001$), and FASN ($p = 0.0007$) compared to age-matched females on NC diet (Fig. 6 and Fig. 2 supplemental). There was no statistical difference between both HFD and NC groups for p-ACL normalized to total ACL protein (p

= 0.22). Also, p-ACC/ACC normalization failed to reach significance (p = 0.44 between NC and HFD). There was a significant increase in IL1B protein expression (p = 0.0006) as well as a decrease in MnSOD (p = 0.043) indicating that the HFD induced liver inflammation and may suppress antioxidant expression. Densitometric analysis was performed with GAPDH as a housekeeping protein on all blots using all liver samples from DIO (n = 23) and NC (n = 10).

Discussion

Several studies indicate that hyperuricemia (high UA levels) is a strong independent predictor of obesity [1–6]. Specifically, two independent untargeted metabolomics studies revealed that circulating UA is the most significantly associated metabolite increased in obesity [24, 25]. Hyperuricemia is not only limited to the pathogenesis of gout, but recent evidence also suggests that hyperuricemia contributes to the pathogenesis of insulin resistance and metabolic syndrome [26–29]. Epidemiologic studies support an association between hyperuricemia and NAFLD [6, 13, 30–44] and data support that elevated levels of circulating UA increases the risk of NAFLD [42–44]. Although these epidemiologic studies examined both males and females while interpreting their data, in many studies the number of males was much greater than females. In addition, very few pre-clinical studies examine the effects of hyperuricemia in female mice affirming a considerable need for progress in understanding sex differences in the context of NAFLD and NASH. To this end, in 2014 the National Institutes of Health (NIH) announced that investigators must address sex differences in preclinical-NIH funded studies which has produced a steady increase in the number of publications on sex disparity. However, Lonardo et al. eloquently described that sex differences in NAFLD are lagging behind other areas of research [17], whereas several major risk factors for NAFLD, such as adiposity, inflammation, metabolic syndrome, and type 2 diabetes, have garnered much more attention (*e.g.* greater numbers of publications).

To address this critical gap in knowledge regarding potential differential responses between sexes, we examined DIO in female mice by assessing obesity and its associated comorbidities, with a particular focus on NAFLD and hyperuricemia. Due to the combination of our previously published work with DIO in C57BL/6J male mice (same diet) [15], extensive reports supporting hyperuricemia in obese male mice [7, 9–14] and adherence to the principle of reduction in numbers, we did not include male mice in this study. Despite an increase in weight, impaired glucose tolerance, and indices of NAFLD, we observed that C57BL/6J female mice fed a HFD (60% fat) for 32 weeks do not have significantly elevated circulating UA levels over the lean controls. We previously observed in C57BL/6J male mice on this same 60% HFD that circulating UA levels were 6.16 ± 0.87 mg/dL (20 weeks of HFD) [15], which was also validated by other groups using the same HFD in male mice [13, 14]. It is important to note that significant elevation in circulating UA levels were seen in these two reports at 8 and 18 weeks demonstrating an early and lasting response to DIO with this 60% HFD. Herein, we observed that the circulating UA levels were 0.93 ± 0.03 mg/dL in the female mice on the 60% HFD at week 32, which was not statistically different from normal chow controls (0.83 ± 0.03 mg/dL) (Fig. 3C). At week 23 (an earlier time point), there was no significant difference in plasma UA levels between the two groups (HFD: 0.39 ± 0.03 mg/dL; NC: 0.35 ± 0.03 mg/dL) despite a significant

increase in delta body weight in the female mice (HFD: 28.5 ± 1.2; NC: 9.5 ± 1.0; $p <$ 0.0001, Supplemental Fig. 1).

It is important to note, that male rodent DIO models have increased plasma UA levels [10–13] corroborating the tight association between elevated UA levels and male obesity as well as its attendant metabolic consequences. Specific to our observations herein, we have previously observed UA levels greater than 6 mg/dL in male C57BL/6J mice at 20 weeks on the same 60% HFD [15] used in this study. These DIO female mice demonstrated that circulating UA levels (HFD: 0.39 ± 0.03 mg/dL) were not significantly elevated at 23 weeks compared to NC (Supplemental Fig. 1). It is important to consider that there is a 15.8-fold difference in plasma UA levels between male and female mice on the same HFD diet despite similiar weight gain. In addition, this positive association between obesity and UA levels in male mice has also been reported in genetic models of obesity in which male obese Pound (leptin receptor deficient) mice show significantly elevated circulating UA levels (> 4-fold) coupled with increased hepatic TG and cholesterol compared to controls [9, 44]. In fact, in many of these reports, this association has extended to causation and is the subject of considerable debate in the field affirming the significance of the sex disparity findings herein as well as identifying the critical need to examine female responses in the context of UA and metabolic dysfunction.

While we report a significant finding, the absence of hyperuricemia in female DIO, the question remains why? The answer may lie in other reports of sex disparity. For example, it is well known that there is less incidence of cardiovascular disease (CVD) in premenopausal females compared to age-matched males [45]. More importantly, the incidence and severity of CVD dramatically increases in postmenopausal women [45, 46]. Similarly, epidemiological studies indicate that there is a greater incidence of NAFLD in men than women before menopause [47, 48], suggesting estrogen may protect against the development of NAFLD, much like with CVD. However, the mechanism for these protective effects in both NAFLD and CVD is far from being clearly elucidated.

Interestingly, hepatic xanthine oxidase (XO) activity is reported to be 59% greater in mature male rats compared to females whereas ovariectomized mature female rats had a 2-fold increase in hepatic XO enzymatic activity, nearly identical to values observed in the mature males [49]. These observations controlled for the potential of differential uricase activity and demonstrated no difference between the sexes. Surprisingly, treatment of mature males with estradiol did not alter liver XOR activity or UA levels. Somewhat countervailing these findings is a report demonstrating estradiol-mediated diminution of XOR enzymatic activity that was independent of promoter activity [50] suggesting a potential post-transcriptional and/or post-translational regulation. Based on these findings, the protective effects of estrogen may be related to a decrease in XOR enzymatic activity and less circulating UA concentrations; however, there is considerable work to be done to clearly define these processes. Regardless of the impact of estrogen on XOR, the sole source of UA, estrogen signaling is associated with protection from both metabolic syndrome and liver damage in females. However, at week 32, our DIO female mice demonstrated significantly elevated transaminase levels compared to age-matched mice on NC (Fig. 3A). While these mice were ~10 months old, which is ~38 years in human age equivalents, we did not examine or

otherwise control for estrogen levels, these results serve to affirm the need for further study of the impact of estrogen in this model.

In general, *de novo* lipogenesis (DNL) is thought to contribute to NAFLD pathogenesis. Stable isotopic analysis of fatty acid and triacylglycerol flux in subjects with NAFLD confirmed that DNL is a distinct characteristic of NAFLD. There was a significant increase in FA synthesis in individuals with NAFLD compared to control subjects [51]. Definitive results supporting this clinical data from mouse models on a HFD is a bit more controversial. Duarte *et al.* demonstrated with a sophisticated D_2O NMR approach that DNL is actually suppressed in a transgenic male mouse that constitutively expresses *Srebp1a* on a 60% HFD [52]. Other groups have shown that the 60% HFD increases hepatic ACC, FASN, and SCD1 protein expression in male mice suggesting that there may be an increase in DNL [53, 54]. However, very little is known about the expression of proteins in the DNL pathway in female mice on this 60% HFD for 32 weeks. Herein, we show that ACC, p-ACC, ACL, and FASN protein expression are all significantly decreased in the liver of female mice following 32 weeks of 60% HFD feeding. Additionally, there was little to no change in any of the lipogenesis genes measured by qPCR. These findings suggest that DNL is not playing a major role in HFD-induced hepatic steatosis.

While exact pathophysiology of NAFLD is not completely understood, it is well known that both inflammation and cholesterol contribute to NAFLD pathogenesis and/or progression to NASH. Inflammatory qPCR markers in the liver of HFD-fed female mice were all significantly increased compared to the age-matched control mice on NC. Additionally, IL1B protein expression was up. Both hepatic cholesterol and cholesteryl esters were increased 1.9- and 1.6-fold, respectively, in the HFD compared to the NC group. One may speculate that this increase in inflammation, cholesterol, and cholesteryl esters may be a reason for the upregulation of fibrosis markers measured by qPCR.

The importance of the findings herein, as well as the identification of critical avenues of further work, lies squarely with the potential to target XOR and by consequence, UA as a promising therapeutic in NAFLD and/or NASH. For example, in 25 patients with hyperuricemia, febuxostat (an FDA-approved XOR inhibitor that decreases plasma UA levels) treatment for 24 weeks decreased serum ALT and AST levels [10]. Unfortunately, clinical characteristics of NAFLD and/or NASH were not reported [10]; however, XOR inhibitors have been shown to decrease plasma UA levels and suppress the development of NAFLD in preclinical rodent models [10, 11, 13, 43]. These studies serve to incentivize: (1) further exploration of the role of UA in NAFLD/NASH as well as other obesity-related metabolic abnormalities and (2) detailed characterization of the apparent sex disparities identified herein by additional side-by-side male vs. female studies using various obesogenic diets and durations.

Fig. 1S. No difference in plasma UA between HFD-fed female mice compared to normal chow (NC) controls at week 23. Delta weight gain of female mice was recorded (A) and plasma UA concentrations were determined (B) at week 23. The values in the bar graph represent mean ± SEM for liver samples processed from DIO female mice ($n = 23$) and NC ($n = 10$). Significance was determined using an unpaired two-tailed Student's t-test.

Fig. 2S. Western blot for p-ACC, ACC, p-ACL, ACL, FASN, XDH/XO, IL1B, and MnSOD in DIO female mice compared to age-matched NC. In Fig. 6, nine liver samples from NC and HFD were analyzed. Fourteen HFD and one NC liver samples from the female mice remained and presented here. Three NC liver samples (1–3) were used in both gel one and two to normalize the data between gels.

Supplementary Material

Refer to Web version on PubMed Central for supplementary material.

Acknowledgments

This work was supported by National Institute of Health (NIH) R01 DK124510-01 for NKHK; R01 DK124510-01, R01 HL153532-01A1, and AHA for EEK; R21 NS112787 for MAF; R01 AA028436 and P30 DK120531 for GEA; R01 GM125944 and R01 DK112854 for FJS.

Data availability

Data will be made available on request.

References

[1]. Kannel WB, Adrienne Cupples L, Ramaswami R, Stokes J, Kreger BE, Higgins M, Regional obesity and risk of cardiovascular disease; the Framingham study, J. Clin. Epidemiol 44 (2) (1991) 183–190. [PubMed: 1995775]

[2]. Bhole V, Choi JWJ, Woo Kim S, de Vera M, Choi H, Serum uric acid levels and the risk of type 2 diabetes: a prospective study, Am. J. Med 123 (10) (2010) 957–961. [PubMed: 20920699]

[3]. Oyama C, Takahashi T, Oyamada M, Oyamada T, Ohno T, Miyashita M, Saito S, Komatsu K, Takashina K, Takada G, Serum uric acid as an obesity-related indicator in early adolescence, Tohoku J. Exp. Med 209 (3) (2006) 257–262. [PubMed: 16778373]

[4]. Biradar MI, Chiang KM, Yang HC, Huang YT, Pan WH, The causal role of elevated uric acid and waist circumference on the risk of metabolic syndrome components, Int. J. Obes 44 (4) (2020) 865–874.

[5]. Tanaka K, Ogata S, Tanaka H, Omura K, Honda C, Osaka Twin Research G, Hayakawa K, The relationship between body mass index and uric acid: a study on Japanese adult twins, Environ. Health Prev. Med 20 (5) (2015) 347–353.

[6]. Wang H, Wang L, Xie R, Dai W, Gao C, Shen P, Huang X, Zhang F, Yang X, Ji G, Association of serum uric acid with body mass index: a cross-sectional study from Jiangsu Province, China, Iran. J. Public Health 43 (11) (2014) 1503–1509. [PubMed: 26060717]

[7]. Nakagawa T, Hu H, Zharikov S, Tuttle KR, Short RA, Glushakova O, Ouyang X, Feig DI, Block ER, Herrera-Acosta J, et al. , A causal role for uric acid in fructose-induced metabolic syndrome, Am. J. Physiol. Renal Physiol 290 (3) (2006) F625–F631.

[8]. Sánchez-Lozada LG, Tapia E, Bautista-García P, Soto V, Ávila-Casado C, Vega-Campos IP, Nakagawa T, Zhao L, Franco M, Johnson RJ, Effects of febuxostat on metabolic and renal alterations in rats with fructose-induced metabolic syndrome, Am. J. Physiol. Renal Physiol 294 (4) (2008) F710–F718.

[9]. Baldwin W, McRae S, Marek G, Wymer D, Pannu V, Baylis C, Johnson RJ, Sautin YY, Hyperuricemia as a mediator of the proinflammatory endocrine imbalance in the adipose tissue in a murine model of the metabolic syndrome, Diabetes 60 (4) (2011) 1258–1269. [PubMed: 21346177]

[10]. Nishikawa T, Nagata N, Shimakami T, Shirakura T, Matsui C, Ni Y, Zhuge F, Xu L, Chen G, Nagashimada M, et al. , Xanthine oxidase inhibition attenuates insulin resistance and diet-induced steatohepatitis in mice, Sci. Rep 10 (1) (2020) 815. [PubMed: 31965018]

[11]. Nakatsu Y, Seno Y, Kushiyama A, Sakoda H, Fujishiro M, Katasako A, Mori K, Matsunaga Y, Fukushima T, Kanaoka R, et al. , The xanthine oxidase inhibitor febuxostat suppresses development of nonalcoholic steatohepatitis in a rodent model, Am. J. Physiol. Gastrointest. Liver Physiol 309 (1) (2015) G42–G51. [PubMed: 25999428]

[12]. Wan X, Xu C, Lin Y, Lu C, Li D, Sang J, He H, Liu X, Li Y, Yu C, Uric acid regulates hepatic steatosis and insulin resistance through the NLRP3 inflammasome-dependent mechanism, J. Hepatol 64 (4) (2016) 925–932. [PubMed: 26639394]

[13]. Xu C, Wan X, Xu L, Weng H, Yan M, Miao M, Sun Y, Xu G, Dooley S, Li Y, et al. , Xanthine oxidase in non-alcoholic fatty liver disease and hyperuricemia: one stone hits two birds, J. Hepatol 62 (6) (2015) 1412–1419. [PubMed: 25623823]

[14]. Zhang X, Nie Q, Zhang Z, Zhao J, Zhang F, Wang C, Wang X, Song G, Resveratrol affects the expression of uric acid transporter by improving inflammation, Mol. Med. Rep 24 (2) (2021) 564. [PubMed: 34109437]

[15]. Harmon DB, Mandler WK, Sipula IJ, Dedousis N, Lewis SE, Eckels JT, Du J, Wang Y, Huckestein BR, Pagano PJ, et al. , Hepatocyte-specific ablation or whole–body inhibition of xanthine oxidoreductase in mice corrects obesity-induced systemic hyperuricemia without improving metabolic abnormalities, Diabetes 68 (6) (2019) 1221. [PubMed: 30936145]

[16]. Tam HK, Kelly AS, Fox CK, Nathan BM, Johnson LA, Weight loss mediated reduction in xanthine oxidase activity and uric acid clearance in adolescents with severe obesity, Child Obes. 12 (4) (2016) 286–291. [PubMed: 26978590]

[17]. Lonardo A, Nascimbeni F, Ballestri S, Fairweather D, Win S, Than TA, Abdelmalek MF, Suzuki A, Sex differences in nonalcoholic fatty liver disease: state of the art and identification of research gaps, Hepatology 70 (4) (2019) 1457–1469. [PubMed: 30924946]

[18]. Khoo NKH, Fazzari M, Chartoumpekis DV, Li L, Guimaraes DA, Arteel GE, Shiva S, Freeman BA, Electrophilic nitro-oleic acid reverses obesity-induced hepatic steatosis, Redox Biol. 22 (2019) 101132. [PubMed: 30769284]

[19]. Kelley EE, Baust J, Bonacci G, Golin-Bisello F, Devlin JE, Croix St CM., Watkins SC, Gor S, Cantu-Medellin N, Weidert ER, et al. , Fatty acid nitroalkenes ameliorate glucose intolerance and pulmonary hypertension in high fat diet-induced obesity, Cardiovasc. Res 101 (3) (2014) 352–363. [PubMed: 24385344]

[20]. Bergheim I, Guo L, Davis MA, Lambert JC, Beier JI, Duveau I, Luyendyk JP, Roth RA, Arteel GE, Metformin prevents alcohol-induced liver injury in the mouse: critical role of plasminogen activator inhibitor-1, Gastroenterology 130 (7) (2006) 2099–2112. [PubMed: 16762632]

[21]. Rusli F, Deelen J, Andriyani E, Boekschoten MV, Lute C, van den Akker EB, Müller M, Beekman M, Steegenga WT, Fibroblast growth factor 21 reflects liver fat accumulation and dysregulation of signalling pathways in the liver of C57BL/6J mice, Sci. Rep 6 (1) (2016) 30484. [PubMed: 27470139]

[22]. Piccinin E, Villani G, Moschetta A, Metabolic aspects in NAFLD, NASH and hepatocellular carcinoma: the role of PGC1 coactivators, Nat. Rev. Gastroenterol. Hepatol 16 (3) (2019) 160–174. [PubMed: 30518830]

[23]. Kohjima M, Higuchi N, Kato M, Kotoh K, Yoshimoto T, Fujino T, Yada M, Yada R, Harada N, Enjoji M, et al. , SREBP-1c, regulated by the insulin and AMPK signaling pathways, plays a role in nonalcoholic fatty liver disease, Int. J. Mol. Med 21 (4) (2008) 507–511. [PubMed: 18360697]

[24]. Cirulli ET, Guo L, Leon Swisher C, Shah N, Huang L, Napier LA, Kirk-ness EF, Spector TD, Caskey CT, Thorens B, et al. , Profound perturbation of the metabolome in obesity is associated with health risk, Cell Metab 29 (2) (2019) 488–500 e482. [PubMed: 30318341]

[25]. Menni C, Migaud M, Kastenmüller G, Pallister T, Zierer J, Peters A, Mohney RP, Spector TD, Bagnardi V, Gieger C, et al. , Metabolomic profiling of long-term weight change: role of oxidative stress and urate levels in weight gain, Obesity 25 (9) (2017) 1618–1624 (Silver Spring, Md). [PubMed: 28758372]

[26]. Xu YL, Xu KF, Bai JL, Liu Y, Yu RB, Liu CL, Shen C, Wu XH, Elevation of serum uric acid and incidence of type 2 diabetes: a systematic review and meta–analysis, Chronic Dis. Transl. Med 2 (2) (2016) 81–91. [PubMed: 29063028]

[27]. Billiet L, Doaty S, Katz JD, Velasquez MT, Review of hyperuricemia as new marker for metabolic syndrome, ISRN Rheumatol. 2014 (2014) 7.

[28]. Cirillo P, Sato W, Reungjui S, Heinig M, Gersch M, Sautin Y, Nakagawa T, Johnson RJ, Uric acid, the metabolic syndrome, and renal disease, J. Am. Soc. Nephrol 17 (12 suppl 3) (2006) S165. [PubMed: 17130256]

[29]. Soltani Z, Rasheed K, Kapusta DR, Reisin E, Potential role of uric acid in metabolic syndrome, hypertension, kidney injury, and cardiovascular diseases: is it time for reappraisal? Curr. Hypertens. Rep 15 (3) (2013) 175–181. [PubMed: 23588856]

[30]. Sirota JC, McFann K, Targher G, Johnson RJ, Chonchol M, Jalal DI, Elevated serum uric acid levels are associated with non-alcoholic fatty liver disease independently of metabolic syndrome features in the United States: liver ultrasound data from the national health and nutrition examination survey, Metabolism 62 (3) (2013) 392–399. [PubMed: 23036645]

[31]. Shih MH, Lazo M, Liu SH, Bonekamp S, Hernaez R, Clark JM, Association between serum uric acid and nonalcoholic fatty liver disease in the US population, J. Formos. Med. Assoc 114 (4) (2015) 314–320. [PubMed: 25839764]

[32]. Ryu S, Chang Y, Kim SG, Cho J, Guallar E, Serum uric acid levels predict incident nonalcoholic fatty liver disease in healthy Korean men, Metabolism 60 (6) (2011) 860–866. [PubMed: 20863537]

[33]. Oral A, Sahin T, Turker F, Kocak E, Relationship between serum uric acid levels and nonalcoholic fatty liver disease in non-obese patients, Medicina 55 (9) (2019) 600 (Mex) (Kaunas). [PubMed: 31533345]

[34]. Wei F, Li J, Chen C, Zhang K, Cao L, Wang X, Ma J, Feng S, Li WD, Higher serum uric acid level predicts non-alcoholic fatty liver disease: a 4-year prospective cohort study, Front. Endocrinol 11 (179) (2020) 1–8.

[35]. Yamada T, Suzuki S, Fukatsu M, Wada T, Yoshida T, Joh T, Elevated serum uric acid is an independent risk factor for nonalcoholic fatty liver disease in Japanese undergoing a health checkup, Acta Gastroenterol. Belg 73 (1) (2010) 12–17. [PubMed: 20458845]

[36]. Keenan T, Blaha MJ, Nasir K, Silverman MG, Tota-Maharaj R, Carvalho JAM, Conceição RD, Blumenthal RS, Santos RD, Relation of uric acid to serum levels of high-sensitivity C-reactive protein, triglycerides, and high-density lipoprotein cholesterol and to hepatic steatosis, Am. J. Cardiol 110 (12) (2012) 1787–1792. [PubMed: 22975466]

[37]. Lee K, Relationship between uric acid and hepatic steatosis among Koreans, Diabetes Metab. 35 (6) (2009) 447–451. [PubMed: 19879789]

[38]. Li Y, Xu C, Yu C, Xu L, Miao M, Association of serum uric acid level with non-alcoholic fatty liver disease: a cross-sectional study, J. Hepatol 50 (5) (2009) 1029–1034. [PubMed: 19299029]

[39]. Kuo CF, Yu KH, Luo SF, Chiu CT, Ko YS, Hwang JS, Tseng WY, Chang HC, Chen HW, See LC, Gout and risk of non-alcoholic fatty liver disease, Scand. J. Rheumatol 39 (6) (2010) 466–471. [PubMed: 20560813]

[40]. Petta S, Cammà C, Cabibi D, Di Marco V, Craxì A, Hyperuricemia is associated with histological liver damage in patients with non-alcoholic fatty liver disease, Aliment. Pharmacol. Ther 34 (7) (2011) 757–766. [PubMed: 21790685]

[41]. Lonardo A, Loria P, Leonardi F, Borsatti A, Neri P, Pulvirenti M, Verrone AM, Bagni A, Bertolotti M, Ganazzi D, et al. , Fasting insulin and uric acid levels but not indices of iron metabolism are independent predictors of non-alcoholic fatty liver disease. A case-control study, Dig. Liver Dis 34 (3) (2002) 204–211. [PubMed: 11990393]

[42]. Xu C, Yu C, Xu L, Miao M, Li Y, High serum uric acid increases the risk for nonalcoholic fatty liver disease: a prospective observational study, PLoS One 5 (7) (2010) e11578. [PubMed: 20644649]

[43]. Sanchez-Lozada LG, Andres-Hernando A, Garcia-Arroyo FE, Cicerchi C, Li N, Kuwabara M, Roncal-Jimenez CA, Johnson RJ, Lanaspa MA, Uric acid activates aldose reductase and the polyol pathway for endogenous fructose and fat production causing development of fatty liver in rats, J. Biol. Chem 294 (11) (2019) 4272–4281. [PubMed: 30651350]

[44]. Lanaspa MA, Sanchez-Lozada LG, Choi YJ, Cicerchi C, Kanbay M, Roncal-Jimenez CA, Ishimoto T, Li N, Marek G, Duranay M, et al. , Uric acid induces hepatic steatosis by generation

of mitochondrial oxidative stress: potential role in fructose-dependent and -independent fatty liver, J. Biol. Chem 287 (48) (2012) 40732–40744. [PubMed: 23035112]

[45]. Mendelsohn ME, Karas RH, The protective effects of estrogen on the cardiovascular system, N. Engl. J. Med 340 (23) (1999) 1801–1811. [PubMed: 10362825]

[46]. Iorga A, Cunningham CM, Moazeni S, Ruffenach G, Umar S, Eghbali M, The protective role of estrogen and estrogen receptors in cardiovascular disease and the controversial use of estrogen therapy, Biol. Sex Differ 8 (1) (2017) 33 33.

[47]. Ballestri S, Nascimbeni F, Baldelli E, Marrazzo A, Romagnoli D, Lonardo A, NAFLD as a sexual dimorphic disease: role of gender and reproductive status in the development and progression of nonalcoholic fatty liver disease and inherent cardiovascular risk, Adv. Ther 34 (6) (2017) 1291–1326. [PubMed: 28526997]

[48]. DiStefano JK, NAFLD and NASH in postmenopausal women: implications for diagnosis and treatment, Endocrinology 161 (10) (2020) 1–12.

[49]. Levinson DJ, Chalker D, Rat hepatic xanthine oxidase activity, Arthritis Rheumatol. 23 (1) (1980) 77–82.

[50]. Budhiraja R, Kayyali US, Karamsetty M, Fogel M, Hill NS, Chalkley R, Finlay GA, Hassoun PM, Estrogen modulates xanthine dehydrogenase/xanthine oxidase activity by a receptor-independent mechanism, Antioxid. Redox Signal 5 (6) (2003) 705–711. [PubMed: 14588143]

[51]. Lambert JE, Ramos–Roman MA, Browning JD, Parks EJ, Increased de novo lipogenesis is a distinct characteristic of individuals with nonalcoholic fatty liver disease, Gastroenterology 146 (3) (2014) 726–735. [PubMed: 24316260]

[52]. Duarte JAG, Carvalho F, Pearson M, Horton JD, Browning JD, Jones JG, Burgess SC, A high-fat diet suppresses de novo lipogenesis and desaturation but not elongation and triglyceride synthesis in mice, J. Lipid Res 55 (12) (2014) 2541–2553. [PubMed: 25271296]

[53]. Xu J, Lloyd DJ, Hale C, Stanislaus S, Chen M, Sivits G, Vonderfecht S, Hecht R, Li YS, Lindberg RA, et al. , Fibroblast growth factor 21 reverses hepatic steatosis, increases energy expenditure, and improves insulin sensitivity in diet-induced obese mice, Diabetes 58 (1) (2009) 250–259. [PubMed: 18840786]

[54]. Kim YR, Lee EJ, Shin KO, Kim MH, Pewzner-Jung Y, Lee YM, Park JW, Futerman AH, Park WJ, Hepatic triglyceride accumulation via endoplasmic reticulum stress-induced SREBP-1 activation is regulated by ceramide synthases, Exp. Mol. Med 51 (11) (2019) 1–16.

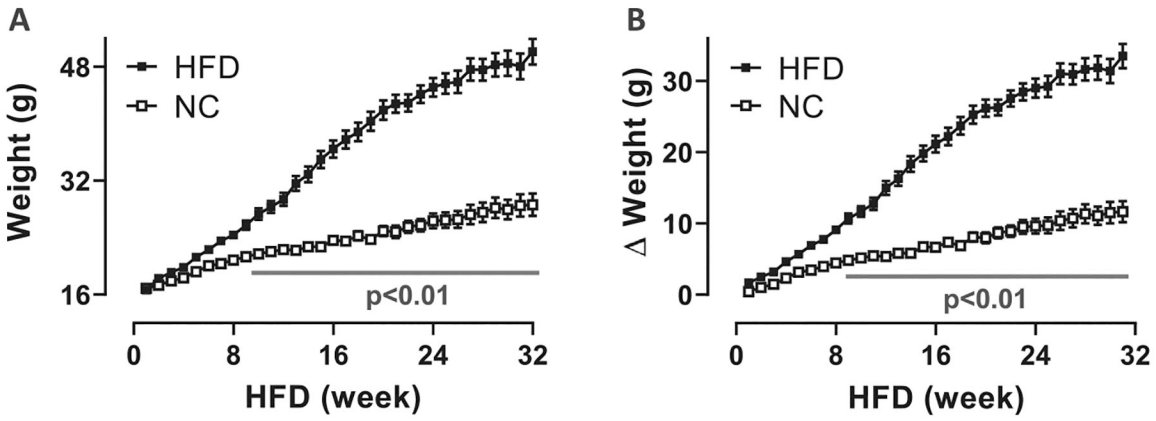

Fig. 1.

C57Bl/6j female mice gain weight on HFD (60 kcal% Fat). Absolute weight of mice fed HFD (n = 23) and NC (n = 10) over 32 weeks (**A**). Delta weight gain plotted over 32 weeks (**B**). Every timepoint is the mean ± SEM (n = 10 to 23 mice). Significance was reached at week 9 between HFD vs NC and determined with 2-way ANOVA using Šídák's multiple comparisons test.

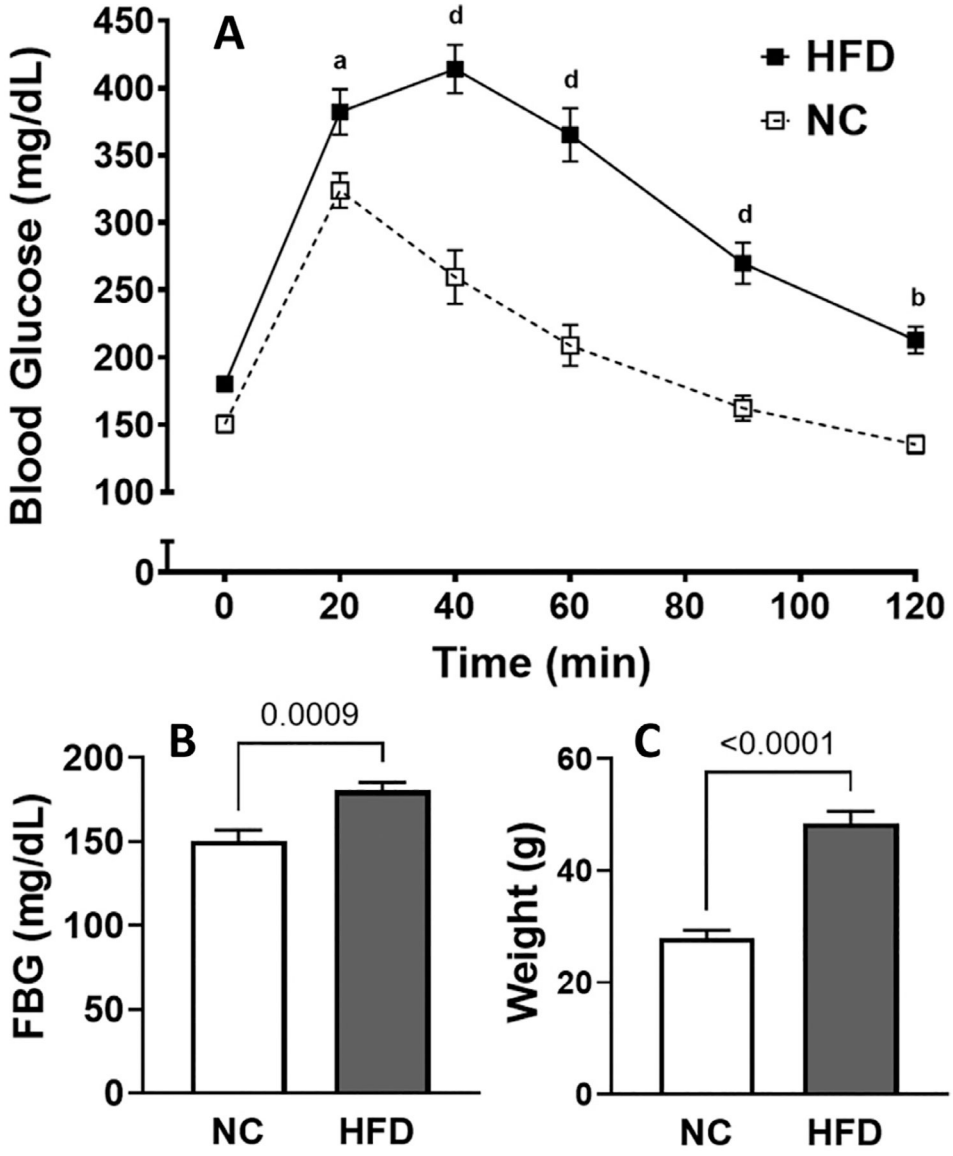

Fig. 2.

HFD-fed mice have impaired glucose tolerance. GTT was performed at week 30 (**A**). Fasting blood glucose levels were recorded at $t = 0$ of GTT (**B**). Weight of mice were recorded on the day of GTT (**C**). Every time-point is the mean ± SEM ($n = 10$ to 23 mice). For GTT, 2-way ANOVA was performed using Šídák's multiple comparisons test (**a**, $p = 0.039$, **b**, $p = 0.002$ and **d**, $p < 0.0001$ vs NC). For FBG and weight, significance was determined using an unpaired two-tailed Student's t-test.

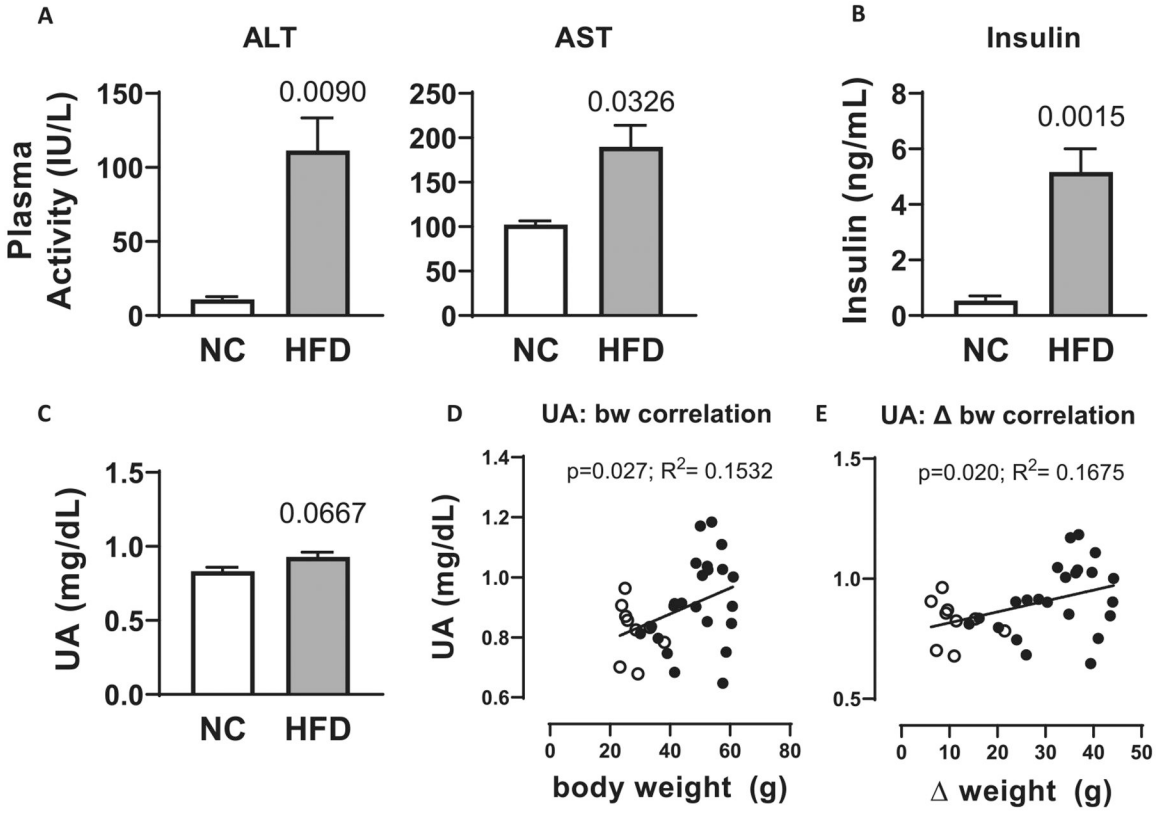

Fig. 3.

HFD-fed mice have increased circulating ALT, AST and insulin. Plasma from the terminal blood draw was used to measure ALT and AST (**A**) as well as circulating insulin levels (**B**). Plasma UA concentrations were measured using reverse-phase high-performance liquid chromatograph (**C**). Pearson correlation was used to test the relationships between circulating UA concentrations and absolute weight (**D**) and delta weight gain (**E**). Data are the mean ± SEM. Significance was determined using an unpaired two-tailed Student's t-test.

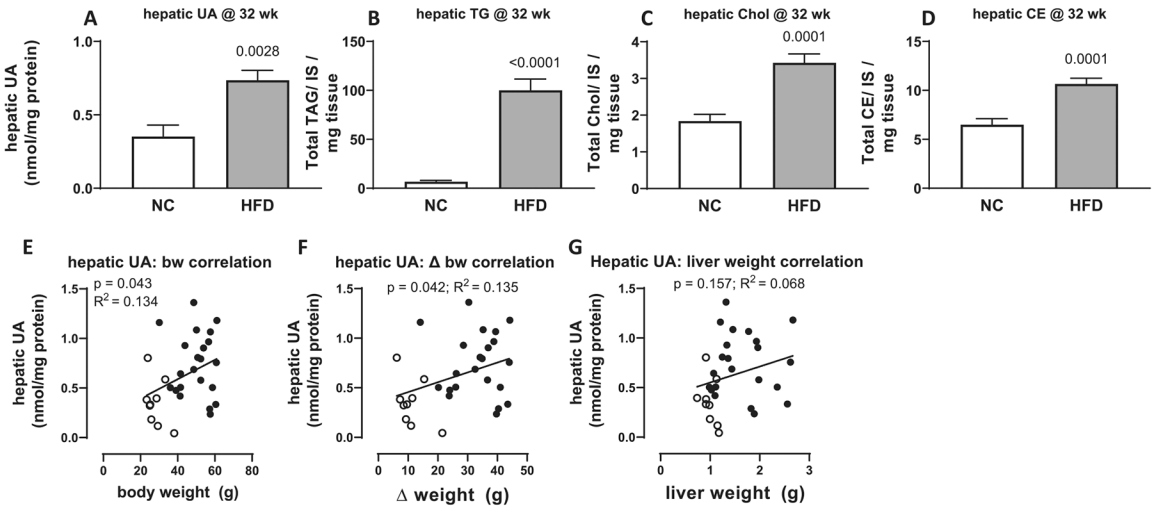

Fig. 4.

HFD-fed mice have increased hepatic UA and TG levels. Hepatic UA concentrations were measured using reverse-phase high-performance liquid chromatograph (**A**). Hepatic TG levels were determined using a HPLC-ESI-MS/MS method (**B**). Hepatic cholesterol (**C**) and cholesteryl ester (**D**) were measured with HPLC-MS/MS methods. Pearson correlation was used to test the relationships between hepatic UA concentrations versus absolute weight (**E**), delta weight gain (**F**), and liver weight (**G**). Data are the mean ± SEM. Significance was determined using an unpaired two-tailed Student's t-test.

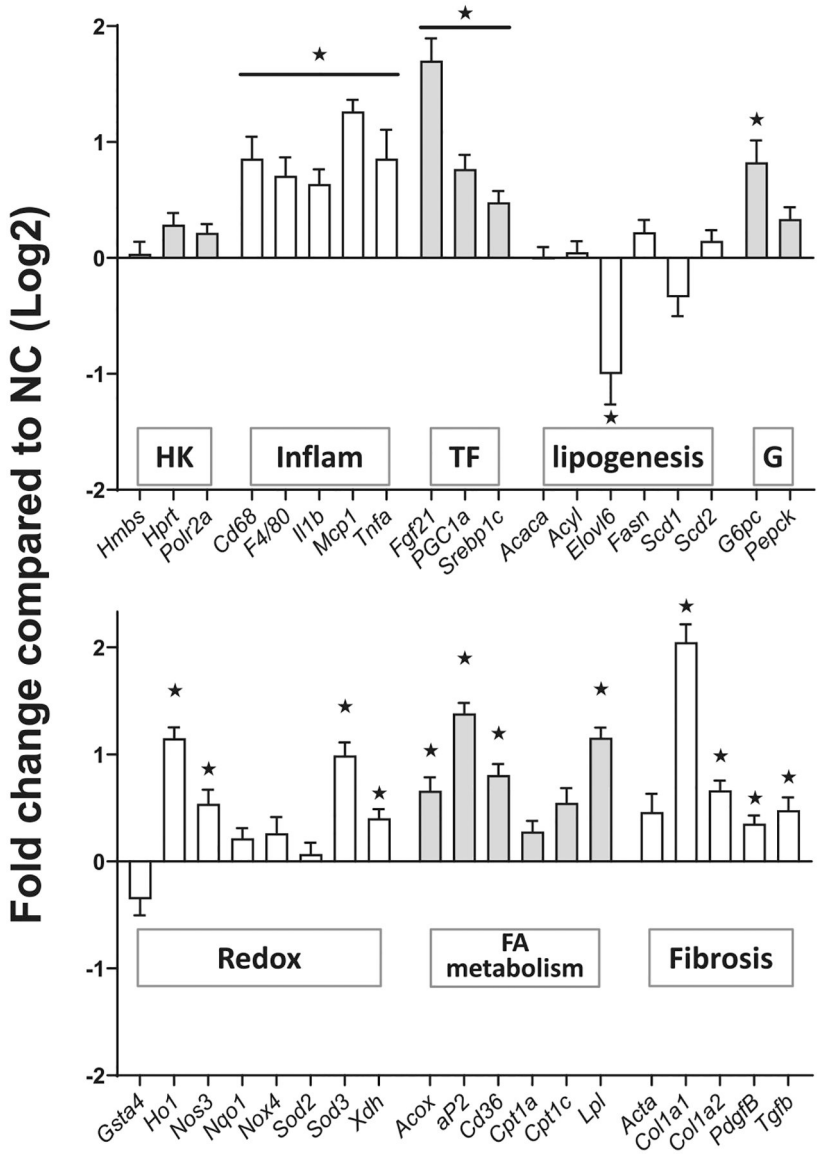

Fig. 5.

Hepatic expression profile of mRNA transcripts associated with inflammation, lipogenesis, gluconeogenesis, redox/antioxidant, fatty acid metabolism, and fibrosis. Hepatic mRNA transcripts from female DIO mice are expressed as fold changes in log2 normalized to the age-matched NC. Actin was used for normalization as it was deemed the most stable gene between all HFD and NC liver samples (see methods). *Hmbs*, Hprt, and *Polr2a* were the other housekeeping genes tested and listed under the abbreviation HK. Additional abbreviations: Inflammation (Inflam), hepatic transcription factor (TF), hepatic gluconeogenesis (G), and fatty acid (FA) metabolism. Data are the mean ± SEM. Significance was determined using an unpaired two-tailed Student's t-test.

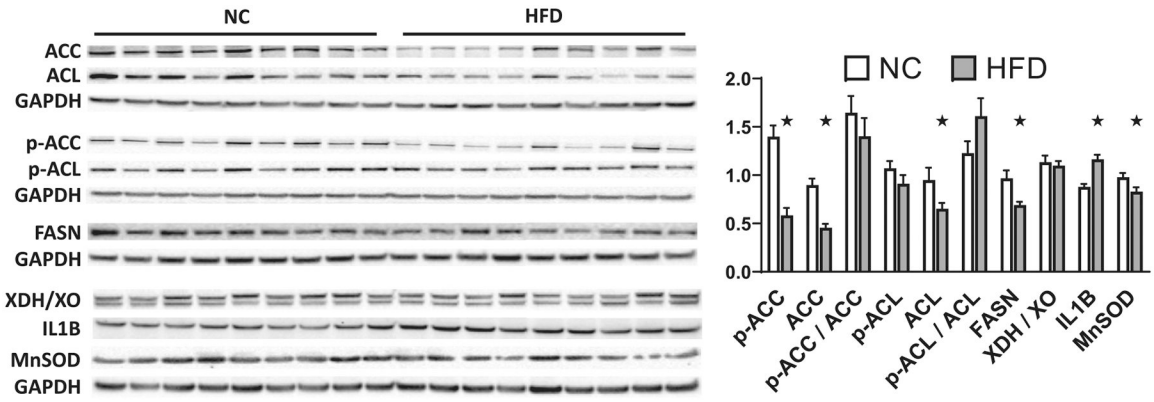

Fig. 6.

Female mice fed a HFD have decreased ACC, A CL, *F* ASN, *and MnSOD protein expression*. Representative western blots for p-ACC, ACC, p-ACL, ACL, FASN, XDH/XO, IL1B, and MnSOD in DIO female mice compared to age-matched NC. The values in the bar graph represent mean ± SEM for liver samples processed from DIO female mice ($n = 23$) and NC ($n = 10$).